11-2020

PLGA-Coated Drug-Loaded Nanotubes Anodically Grown on Nitinol

F. Davoodian
K. N. Toosi University of Technology

E. Salahinejad
K.N.Toosi University of Technology

E. Sharifi
Hamadan University of Medical Sciences

Z. Barabadi
Hamadan University of Medical Sciences

Lobat Tayebi
Marquette University, lobat.tayebi@marquette.edu

Materials Science and Engineering : C, Vol. 116 (November 2020): 111174. DOI.

PLGA-Coated Drug-Loaded Nanotubes Anodically Grown on Nitinol

F. Davoodian
Faculty of Materials Science and Engineering, K. N. Toosi University of Technology, Tehran, Iran
E. Salahinejad
Faculty of Materials Science and Engineering, K. N. Toosi University of Technology, Tehran, Iran
E. Sharifi
Department of Tissue Engineering and Biomaterials, School of Advanced Medical Sciences and Technologies, Hamadan University of Medical Sciences, Hamadan, Iran
Z. Barabadi
Department of Tissue Engineering and Biomaterials, School of Advanced Medical Sciences and Technologies, Hamadan University of Medical Sciences, Hamadan, Iran
L. Tayebi
Marquette University School of Dentistry, Milwaukee, WI

Abstract

This study evaluates the use of nanotubes (NTs) as a matrix for local drug delivery modified by a biodegradable polymeric coating on medical-grade nitinol (NiTi alloy) surfaces. For this purpose, NiTi

was anodized within parameters that promote the formation of NTs, ultrasonicated, annealed and impregnated with vancomycin hydrochloride. To improve bioperformance, poly(lactic-co-glycolic acid) (PLGA) was also deposited on the drug-loaded NTs. The samples were characterized in terms of structure, wettability, drug delivery, corrosion and cytocompatibility. Scanning electron microscopy and water contact angle measurements signify the formation of open-top homogeneous NTs of 600–700 nm in length and ~30 nm in diameter with improved hydrophilicity. The bare antibiotic-impregnated NTs exhibit a burst release of about 49% of the loaded drug in the first 6 h of soaking in a physiological medium, followed by the entire drug diffusing out before 96 h. The PLGA coating effectively controls the burst release of vancomycin to 26% and retains almost 50% of the loaded drug beyond 7 days. The kinetics of the different vancomycin-release stages is also correlated to several well-established models. As a comparative criterion of metallic ions leaching kinetics, the corrosion resistance of nitinol is found to be reduced by the formation of the NTs, while the PLGA coating enhances this electrochemical feature. Due to the alteration of the drug delivery and corrosion protection, the PLGA-coated vancomycin-impregnated sample presents a higher dental pulp stem cell viability in comparison to both the bare drug-loaded and non-loaded NTs. In conclusion, PLGA-coated vancomycin-loaded NT-covered NiTi can be effectively used as a controlled drug-delivery device, while having a drug-release dosage within the therapeutic window and a minimal negative effect on biocompatibility.

Keywords

Shape-memory alloys, Surface engineering, Wetting, Aliphatic polyester, Glycopeptide antibiotic, Biomedical applications

1. Introduction

Nearly-equiatomic NiTi alloy has long been under consideration for further development and expansion of biomedical applications, especially in orthopedics that exploit a unique combination of mechanical properties (shape-memory effect, low stiffness, high fatigue and wear resistance) and decent biocompatibility of this alloy [[1], [2], [3]]. Nevertheless, orthopedic operations involving implants are generally prone to post-surgery infections, a serious condition that can lead to morbidity, the need for revision surgery and in severe cases even mortality [4] unless addressed therapeutically.

The classical approach for infection prevention at the implantation sites is the prolonged, high-dose intravenous systemic antibiotic administration which bears several well-documented shortcomings, such as poor antibiotic biodistribution, uncontrollable pharmacokinetics and serious side effects for non-target organs [5,6]. An alternative approach for infection prophylaxis in implanting operations is the employment of local drug-delivery strategies, ranging from antibiotic-loaded poly(methyl methacrylate) beads and bone cements [7,8] to drug-impregnated surface-modified titanium alloy implants in which anodically-grown nanotubes (NTs) act as drug reservoirs [[9], [10], [11], [12]].

Drug-loaded NTs on titanium alloys have shown the ability to satisfy the requirements of successful local drug-delivery devices, in terms of effective therapeutic drug doses continually delivered to the target site over prolonged periods [13,14]. Nonetheless, drug-loaded NTs are notorious for the rapid release of their therapeutic load [15,16] since it can lead to adverse effects, e.g. the drug toxicity and the inability to sustained long-term drug release. Different solutions have been explored to control the

drug-release rate from these NTs. Applying biodegradable polymer coatings is one of the most effective approaches in modulating the drug-release kinetics from NTs. To do so, chitosan and poly(lactic-*co*-glycolic acid) (PLGA) are top candidates because both are highly biocompatible and have shown an antibacterial ability along with improved osseointegration [9].

Anodization in fluoride-containing electrolytes is a common approach for the fabrication of geometrically tunable NTs on the surface of titanium and its alloys [17]. This approach has been successfully extended for the formation of NTs on other Ti-X alloys with varying success [18,19] that mainly depends on the type and concentration of alloying element. For example, NTs can be anodically produced on Ti__Zr alloys in a wide range of Zr concentrations as Zr is a valve metal. In contrast, the anodic fabrication of NTs on Ti__Ru alloys is limited at Ru contents higher than 5 at.% since non-valve Ru lacks the ability to form a compact passive layer upon reaction with oxygen. In case of nearly-equiatomic NiTi alloy having a high concentration of non-valve Ni, anodization in fluoride-containing electrolytes has been proven to produce NTs [[20], [21], [22]], albeit in a narrow range of fabrication parameters compared to Ti.

To the best of our knowledge, there is no report in the literature on the drug impregnation of NTs grown on NiTi alloy. In this study, NTs are fabricated on the surface of NiTi alloy by anodization in an electrolyte reported elsewhere [22,23] to assess the feasibility of using NTs as a platform for the controlled local delivery of a model antibiotic agent for the first time in the relative literature. Vancomycin hydrochloride, a highly water-soluble glycopeptide antibiotic which is commonly prescribed for the treatment of osteomyelitis caused by *Staphylococcus aureus* gram-positive bacteria [24] was selected as the model drug for incorporation into the NTs grown on NiTi. PLGA coating on the drug-loaded NTs is also followed to modulate the drug-release kinetics as this biopolymer is more versatile than chitosan in terms of tuning its degradation rate and its chain's relative hydrophilicity/hydrophobicity. In PLGA, lactic (less hydrophilic chains) to glycolic (more hydrophilic chains) monomer ratio determines the polymer's water-uptake, influencing its degradation rate [[25], [26], [27]]. Based on these assumptions, PLGA 75:25 is selected for its longer degradation rate and higher hydrophobicity, which can further delay the diffusion of highly hydrophilic vancomycin molecules. The prepared samples are afterwards compared from drug-delivery, corrosion and cell cytocompatibility viewpoints.

2. Materials and methods

2.1. Materials

The materials used in this study include medical-grade Ni__50Ti disks (Kellogg's Research Labs, USA) of 9 mm in diameter as the substrates, ethylene glycol (Reag. USP grade, Merck, Germany) and ammonium fluoride (ACS grade, Merck, Germany) as the anodization electrolyte, vancomycin hydrochloride (molecular biology grade, Alfa Aesar, USA) as the incorporating drug, double-distilled water (purity: 99%, conductivity: 1 $\mu s \cdot cm^{-1}$) as the solvent and PLGA (LA/GA ratio: 75:25, acid-terminated, Corbion, Netherlands) as the coating agent.

2.2. Fabrication of NTs

The NiTi disks were first ground, polished and washed under ultrasonication in ethanol and distilled water. The non-working side of the disks was coupled to a copper wire via copper tapes and sealed

with silicone rubber. Each of the surface-processed samples were anodized in 100 ml of an ethylene glycol-based electrolyte containing 0.2 wt% NH_4F and 1 vol% H_2O at 25 V for 60 min, in accordance with Refs. [18,28], in a two-electrode cell with a cathodic Pt sheet of $12 * 12$ mm^2 in area at room temperature. The distance between the cathode and the working electrode was set at 20 mm. In order to remove debris from the formed NT tops, ultrasonic cleaning in successive ethanol and distilled water for 5 and 10 min was also conducted. The samples were also heat-treated at 600 °C for 1 h with the heating and cooling rate of 3 °C/min under vacuum, based on Refs. [28, 29], to ensure an optimal combination of wettability, biocompatibility, corrosion and bioactivity characteristics. Typically, the employed annealing temperature has been reported to retain the superelasticity and shape-memory characteristics of NiTi [30], giving transformation temperatures appropriate for biomedical applications [31]. The morphology of the samples was investigated by a field-emission scanning electron microscope (FESEM, TESCAN, MIRA 3).

2.3. Wettability measurement

For wettability studies, the sessile water drop technique was used by pipetting five microliters of double-distilled water on the samples. The ImageJ software was used to measure the contact angle between the drop contour and software-defined baseline. The procedure was repeated three times on different surface spots of the samples and the average values were reported.

2.4. Antibiotic loading and PLGA coating

The annealed samples were loaded with vancomycin as a model antibiotic drug via the setup of Ref. [32]. In summary, one sample was put in a 15 ml falcon tube with a bore in its plastic cap. The falcon tube was placed upside-down in a 250 ml round-bottom flask. After the flask evacuation for 30 min, a 10 mg/ml vancomycin aqueous solution was introduced to the setup and left for 24 h to ensure the maximum drug molecule adsorption on NT walls. Subsequently, the samples were dried at room temperature for 24 h in air.

The drug-loaded samples were cleaned with a soft tissue and rinsed with the phosphate buffer saline (PBS) solution briefly to remove any excess drug from the surface before polymer coating. Afterwards, the drug-loaded samples were dipped in a 1% (w/v) PLGA solution dissolved in acetone with the immersion time of 10 s. Then, the samples were dried at 50 °C for 15 min.

2.5. Drug-release characterization

The release of vancomycin from the bare and PLGA-coated drug-loaded samples was investigated by immersing the samples in 10 ml of PBS at 37 °C. At intervals of 1, 3, 6, 9, 12, 24, 48, 72, 96, 120, 144 and 168 h, 4 ml of the medium was taken and refreshed. The amount of the drug released into the PBS was measured by ultraviolet-visible spectroscopy (UV–vis, Perkin Elmer, Lambda 14) with a resolution of 1 nm at 280 nm. The drug concentration was calculated from calibration curves obtained for known vancomycin concentrations in PBS. The total amount of the loaded drug was also determined when the UV–vis spectra showed no further absorbance changes at 280 nm. The measured experimental data was also further analyzed by fitting with several well-established drug-delivery models, where the goodness-of-fit was determined based on the closeness of linear correlation coefficient (R_c) to the unit.

2.6. Corrosion studies

The open circuit potential (OCP) of the samples in the PBS solution at 37 °C was recorded. After reaching a steady-state OCP (2 h), potentiodynamic polarization was conducted with a scan rate of 1 mV/s in a potential range of −0.8 V to +1.5 V, using a potentiostat (Radstat 10, Kianshar Danesh Co.) with a Pt counter electrode and AgCl/Ag reference electrode at 37 °C. The exposed surface area of the samples in the corrosion studies was equal to 0.635 cm^2.

2.7. In vitro cytocompatibility assessment

The MTT assay was performed to determine the dental pulp stem cell (DPSC) viability on the samples. Each experiment was performed in triplicate at the specified culture durations of 1, 3 and 7 days in a 48-well plate, as reported previously [33] with some modifications. At the desired periods, the culture medium was removed, and 100 µl of 0.5 mg/ml MTT solution in the medium was added to each well and incubated for 4 h at 37 °C. Thereafter, 100 µl of dimethyl sulfoxide (DMSO) solution was added to each well to dissolve formazan crystals. Finally, the solution was transferred to a 96-well plate to determine the optical density values at the wavelength of 545 nm using a microplate reader (ChroMate-4300, FL, USA). The one-way analysis of variance (ANOVA) with a statistical significance level of <5% (p-value < 0.05) was used to compare the cytocompatibility data.

3. Results and discussion

3.1. Morphological studies

Fig. 1(a) represents the FESEM micrograph of the as-anodized sample. NTs are not completely evident in this sample because their tops are covered by debris and precipitates from the electrolyte [34], which makes these NTs unsuitable for drug loading due to the blockage of the matrix. To clean the NT tops from these deposits, anodization was followed by ultrasonication. Since there is no information in the literature, to our knowledge, on optimized conditions under which sonication of anodized NiTi produces open-top NTs, two sonication processes were experimented. Based on Fig. 1(b), sonication for 5 min (2.5 min in ethanol and 2.5 min in distilled water) successfully develops open-top NTs via the desorption of the physically deposited debris. This sample also exhibits a homogenous feature of NTs grown over the whole investigated area with minimal damage. Although by increasing sonication to 10 min (5 min in ethanol and 5 min in distilled water) a precipitate-free surface is still obtained, the excess energy provided by longer sonication results in the damage and removal of NTs from some areas, according to Fig. 1(c). Therefore, it is concluded that the optimized duration of sonication is 5 min to achieve open-top non-detached NTs. Thereafter, the anodized samples for further studies are processed with the mentioned parameters to ensure a maximum drug loading capacity.

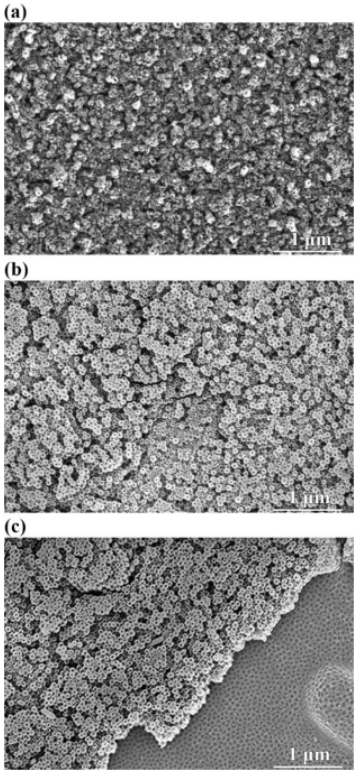

Fig. 1. FESEM micrograph of the samples processed by anodization (a), anodization followed by sonication for 5 min (b) and anodization followed by sonication for 10 min (c).

The anodized, sonicated NiTi samples were heat-treated at 600 °C for three purposes. First, anodization in fluoride-containing electrolytes has been reported to leave organic residues like $[TiF_4]^{2-}$ on the surface. This not only decreases the biocompatibility of the device but also increases the bacterial adhesion to the surface disadvantageously, which can be overcome by annealing at above 500 °C [16,35]. Second, previous surface-compositional studies have shown that the annealing scheme applied in this work decreases the level of Ni from 2.15 at.% to 1.90 at.%, which is accompanied by a reduction of the Ni/Ti ratio from 0.23 to 0.13 [28]. This decrease is favorable for long-term biomedical applications of the related devices as it can lead to improved biocompatibility. Third, annealing at 600 °C can beneficially affect the crystallinity of NTs by promoting the formation of the rutile phase [20,36].

Fig. 2(a) and (b) depicts NTs after annealing. As evidenced, the NTs show no morphological collapse after annealing, as compared to Fig. 1(b). The average diameter of the NTs is estimated to be approximately 35 nm, which is within the optimal range for the highest cell differentiation ability [37]. The mean length of the NTs is also measured to be almost 600 nm, based on the tilted view of the sample (Fig. 2(c)). The dimensions of the obtained NTs are consistent with the literature [18,38,39], where there is a limit for the maximum achievable length of anodically-produced NTs on NiTi. This is due to the high concentration of non-valve Ni in NiTi with little potential to form compact oxides upon oxidation unlike valve Ti and also to the higher solubility of nickel oxides compared to titanium oxides in the presence of fluorine [16]. It is also noticeable that the produced NTs exhibit the highest achievable length-to-diameter ratio reported to date, which is critical for a high drug loading capacity and low burst drug release [15,40].

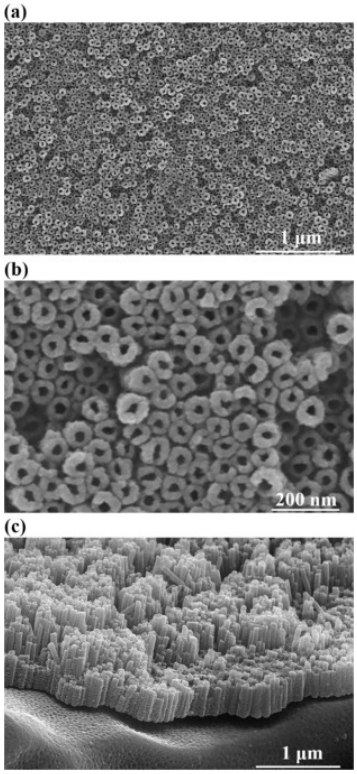

Fig. 2. FESEM micrograph of the sample subjected to the sequence of anodization, sonication and annealing from top views in two magnifications (a, b) and a tilted view (c).

The FESEM micrograph of the drug-loaded NTs before and after PLGA coating is indicated in Fig. 3. From the re-blockage of the NT tops in Fig. 3(a), it is inferred that the drug is successfully penetrated inside the NTs and intertubular spaces with a homogeneous distribution on the whole surface of the disks. Fig. 3(b) also demonstrates the successful uniform deposition of PLGA on the NTs tops, where the depressions of the biopolymer film are indicative of the pore opening structure of the NTs beneath the coating.

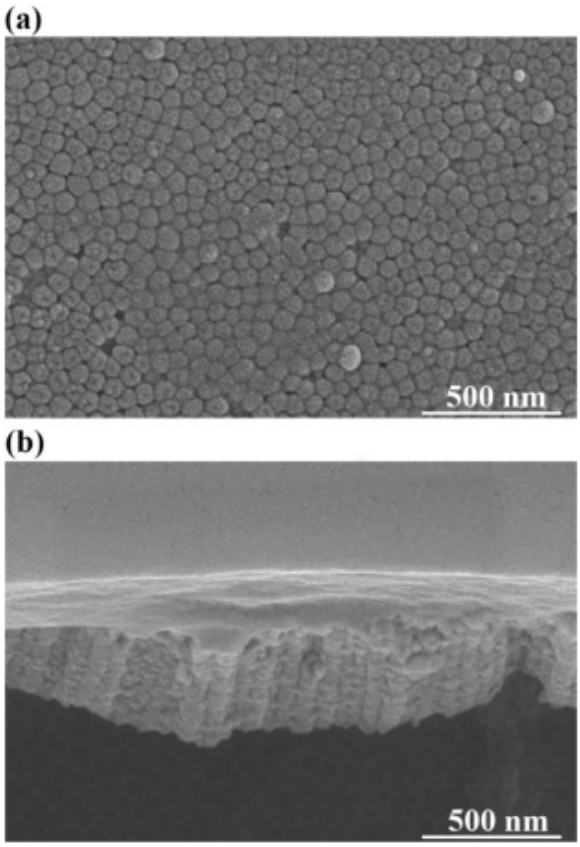

Fig. 3. FESEM micrograph of the NTs loaded with vancomycin from a top view (a) and coated with PLGA from a tilted view (b).

3.2. Water contact angle measurements

The wettability of implants has a determining effect on the protein adsorption, biocompatibility and bioactivity of the devices [29,41]. In this regard, bone/cell adhesion, proliferation and mineralization are found to be promoted by increasing the surface hydrophilicity. In addition, it is logically anticipated that water-soluble drugs like vancomycin have a facilitated and therefore increased incorporation into more hydrophilic matrixes. Fig. 4 signifies the side-view of water drops on the as-ground, as-anodized and annealed samples. The as-ground NiTi sample exhibits a sessile water contact angle of 63.1 ± 2.9°, which is controlled by the naturally-formed oxide layer on its surface [42]. The contact angles measured on the as-anodized and annealed samples are equal to 55.2 ± 3.34° and 43.2 ± 2.7°, respectively. The enhancement in wettability after anodization is attributed to hydroxylation (the formation of surface Ti-OH groups) and roughening. Indeed, the formed NTs and intertubular spaces can allow the liquid penetration and accordingly decrease the contact angle [43]. The further increase of hydrophilicity after annealing is attributed to the crystallization of the NTs. The effect of annealing schemes on the crystallinity of mostly amorphous NTs anodically grown on NiTi has been extensively discussed in the literature, where it has been reported that annealing at 400–500 °C and beyond 550 °C promotes the formation of anatase and rutile crystalline phases, respectively [20,23,29].

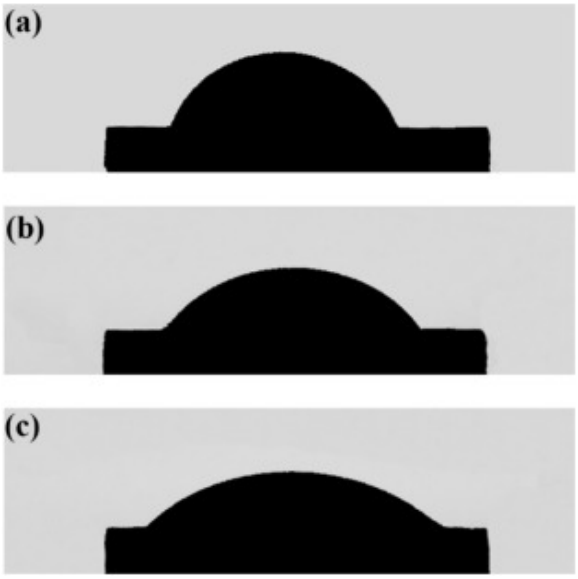

Fig. 4. Side-view macrograph of water drops on the as-ground (a), as-anodized (b) and annealed (c) samples.

3.3. Drug-delivery kinetics studies

The concentration and cumulative percentage of vancomycin released from the devices are revealed in Fig. 5(a) and (b), respectively. Both of the sample sets display a biphasic behavior, including a sharp onset of the drug release during the first 12 h for the bare sample and the first 6 h for PLGA-coated sample, along with a subsequent slower sustained release in the next durations. For the bare NTs, the initial burst release is characterized by about 74.0% of vancomycin into the PBS until 12 h, followed by a slower release of remaining vancomycin until 96 h. The reason behind the initial burst release is postulated to be a steep gradient of the drug concentration at the NTs-PBS interface. It is believed that the drug molecules physically-adsorbed on the NT tops and intertubular spaces which are in immediate contact with the PBS media are released at this stage. The sustained release of vancomycin in the later 84 h is also attributed to the drug molecules deeply-incorporated in the nanotubular structure acting as a stable reservoir of the drug. The drug-delivery kinetics from similarly-sized NTs grown on Ti alloy substrates has been reported to be 100% of release by 6–12 h [15,16,44]. In comparison to the literature, this prolonged release of the drug explored in this work can be due to several reasons. First and foremost, the drug is loaded in the NTs through a vacuum technique in this study, which significantly increases the drug-loading and incorporation levels into the NTs. Capillary forces caused by the small dimensions of NTs and also air molecules residing on the top of NTs during the drug-loading stage limit the amount and depth of the drug penetration into the NTs. Drug-loading techniques like pipetting and immersion used in many previous studies [13,14,45] rely only on the force of gravity and surface adsorption, which results in the partial impregnation of NTs [46]. The vacuum-loading technique not only can counter the air molecules hindering the drug penetration but also provide an additional force to incorporate the drug further in the length of NTs. Another considerable aspect that can affect the drug-loading behavior of the bare NTs is their lowered water contact angle after annealing and crystallization into rutile. Vancomycin is a highly water-soluble drug having a hydrophilic nature, so that water-dissolved vancomycin loading into surfaces can be facilitated by using lower water contact angles. This can result in an easier penetration of drug molecules into the depth of NTs and accordingly a slower release kinetics evidenced in this study. Additionally, annealing

of NTs at 600 °C has been reported to cause the formation of OH^- groups on the surface of NTs [29]. These negatively-charged groups can interact with the naturally-positive charge of vancomycin, leading to a further delay in the drug-release kinetics.

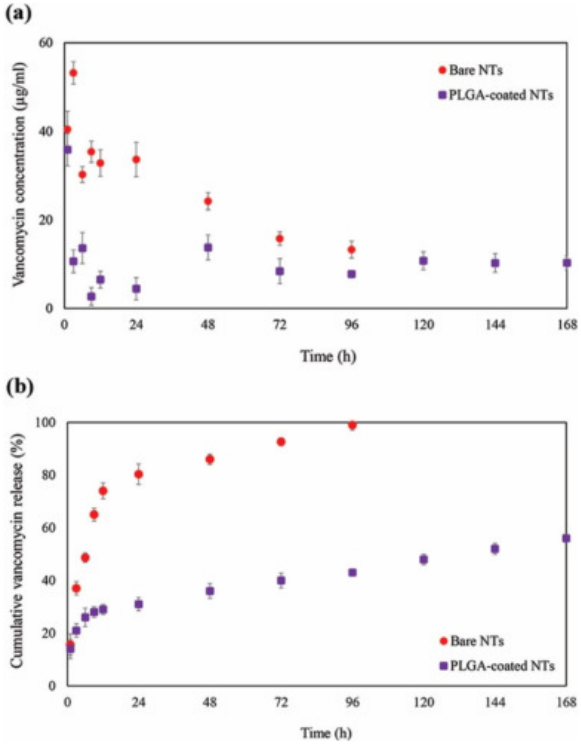

Fig. 5. Concentration (a) and cumulative percentage (b) of the drug released from the devices.

In comparison to the bare NTs, the PLGA coating of the drug matrix provides a substantial alteration in the release kinetics. Under this condition, the burst release in the first 6 h is reduced from 48.6% to 26.0%. Additionally, the polymer-coated sample continues to release vancomycin beyond the 7th day of the release study with only 56.0% release of the total loaded vancomycin amount at the end of the 7th day. Further testing showed that a soaking period of 14 days is required for the entire release of vancomycin loaded. Generally, the release of drugs from polymer-coated surfaces is dependent on the polymer degradability, thickness, permeability and interaction with the diffusing drug [47,48]. PLGA is biodegraded through water uptake and swelling accompanied by the hydrolysis and cleavage of its backbone. When the thin layer of PLGA on the NTs comes in contact with PBS initially, it rapidly starts swelling, thereby leading to a burst release of 26.0%. This is followed by a reduced degradation rate because PLGA used in this work enjoys the specification of LA/GA = 75:25. That is, PLGA with the high LA fraction in its network is less hydrophilic and therefore has a lower hydrolysis degradation rate. Also, due to the presence of more hydrophobic LA monomers, the diffusion of highly hydrophilic drugs such as vancomycin becomes more difficult, resulting in a longer release period. This notion is corroborated by the slowed out-diffusion of vancomycin in the media, which is extended to up to 14 days in the PLGA-coated NTs.

It is vital that the concentration of vancomycin in the medium over the soaking period to be within the therapeutic window for a successful local drug-delivery system. For vancomycin, this translates into meeting the minimum inhibitory concentration (MIC) needed for the effective countering of bone-

related bacterial infections. *S. aureus* are gram-positive bacteria that are responsible for most post-surgery infections and are effectively and routinely countered by the systematic administration of vancomycin after surgeries. Vancomycin has been reported to have a MIC of 1–10 µg/ml, based on in vitro studies conducted on *S. aureus* cultured colonies [16,49]. For both of the samples and the entire drug-release periods, it is seen in Fig. 5(a) that the vancomycin concentration is consistently above the MIC value of *S. aureus*. From this viewpoint, the ability of these local drug-delivery platforms to release an antibacterial agent within its therapeutic window and, in theory, to successfully stop the bacterial proliferation and biofilm formation is realized. Nevertheless, to ensure the control of osteomyelitis, the MIC level should be met for at least two weeks [50], which is not satisfied with the bare NTs. Thus, it is logically anticipated that the PLGA-coated sample provides a safer treatment of osteomyelitis.

To further analyze the drug-delivery kinetics from the bare and PLGA-coated NTs, the experimental vancomycin-release data of both burst and sustained stages was fitted with the Higuchi [51], zero-order [52] and first-order models [53]. Based on Table 1 which lists R_c values, the bare drug-loaded NTs show the best fit with the first-order model during the first 6 h (Fig. 6(a)) and with the Higuchi kinetics during the remaining period of vancomycin release (Fig. 6(b)). The assignment of a burst drug release kinetics for the first 6 h from the bare NTs is in good agreement with the physical basis of the first-order model which is essentially established for a fast and concentration-dependent drug delivery. The following sustained release stage, which was above attributed to the deeply-incorporated remaining drug molecules, is verified by the domination of the diffusion-controlled Higuchi kinetics. The unsuitable fit of the bare sample data with the zero-order kinetics is also due to the much larger diameter of the NTs (~30 nm) than eluting vancomycin molecules (~3 nm) [54].

Table 1. Linear correlation coefficient (R_c) values of the drug-delivery kinetics fits.

Model	**R_c for the bare NTs**		**R_c for the PLGA-coated NTs**	
	Burst stage	**Sustained stage**	**Burst stage**	**Sustained stage**
Higuchi	0.91	0.99	0.98	0.99
First-order	0.99	0.85	0.91	0.87
Zero-order	0.85	0.82	0.89	0.83

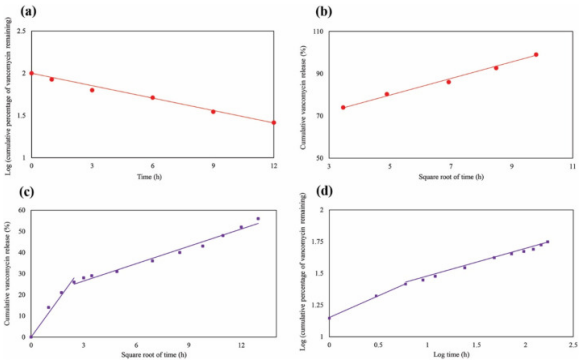

Fig. 6. Drug-release fitting curves of the first-order (a) and Higuchi (b) models for the bare NTs, and the Higuchi (c) and Korsmeyer-Peppas (d) models for the PLGA-coated NTs.

In accordance with Table 1, the vancomycin-release data for the PLGA-coated sample reveals the best fit with the Higuchi kinetics for both the burst and sustained stages. In comparison to the bare NTs, the

transformation of the fast first-order release to the diffusion-controlled Higuchi kinetics for the initial release phase is indicative of the shortening of the burst kinetics as a result of the PLGA coating. The fact that the PLGA-coated NTs continues to have a good fit with the Higuchi kinetics in the sustained phase suggests a diffusion-controlled mechanism of vancomycin release. Biodegradable polymers used as a barrier for controlled drug-delivery applications tend to introduce both diffusion- and degradation-controlled mechanisms to the underlying drug-loaded substrates. The relatively low degradation rate of 75:25 PLGA during the 7-day release study is thought to be the reason for the continued diffusion-controlled mechanism for the polymer-coated sample. To further explore the elution kinetics of the coated sample, the Korsmeyer-Peppas model [53] which can also account for non-Fickian behaviors is employed. The value n in this model can characterize different release mechanisms, so that for thin films $n < 0.5$ indicates a diffusion-controlled mechanism, while $n > 1$ is interpreted as degradation-controlled. Values between these bounds hint at the superposition of both mechanisms. The PLGA-coated sample presents a good fit with the Korsmeyer-Peppas model at both stages, where the values obtained for n are 0.34 for the burst stage and 0.86 for the sustained stage. This implies that the driving force of diffusion is reduced by increasing the elution time, indicating the onset of PLGA degradation which is not yet rapid enough during the 7-day study to dominate the release mechanism.

3.4. Electrochemical corrosion evaluation

The variations of OCP vs. immersion time in PBS and the potentiodynamic polarization curves of the mechanically-ground, as-anodized, annealed, and PLGA-coated samples in terms of potential (E) and current density (i) are presented in Fig. 7. As revealed in Fig. 7(a), for the as-ground sample, the OCP displays a sharp increase at the onset of immersion, followed by stabilization at approximately −0.2 V. Preferential and spontaneous oxidation of Ti atoms in PBS leads to the evolution of an oxide layer on the surface until a balance between oxidation and dissolution is established [29], where the diffusion of oxidizers in the oxide layer is limited by increasing the oxide thickness. The as-anodized samples display a relatively stable potential with a slight increase during 2 h of immersion, which is thought to be due to a compromise of the anodization-assisted formation of an oxide layer and oxidation reactions taking place at defects of the NT layer. Annealing of the NTs increases the OCP to more positive values, due to the further oxidation of the substrate through defects of the NT layer. The PLGA-coated sample is also shown to have a stable OCP, which is attributed to the thin PLGA layer hampering the charge transfer at the electrode/electrolyte interface.

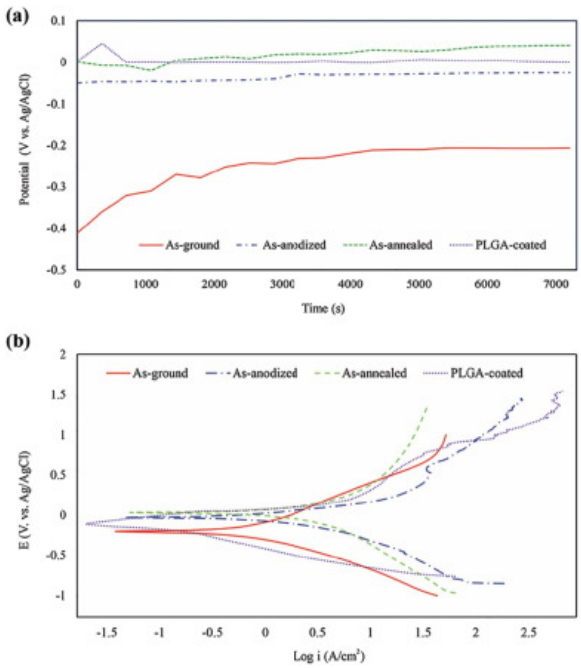

Fig. 7. Open circuit potential (a) and potentiodynamic polarization (b) curves of the samples.

According to the polarization curves (Fig. 7(b)), it is observed that the as-ground sample displays higher corrosion resistance than both of the as-anodized and annealed NT-covered samples. This is consistent with previous reports that show anodization declines corrosion resistance, despite the fact that this process promotes that formation of a thick oxide layer on NiTi [22]. This is attributed to the fact that NTs essentially provide larger surface areas than the naturally-formed oxide layer of the as-ground sample and act as pathways for mass-transport phenomena such as corrosion. Annealing of the NTs at 600 °C is realized to increase the corrosion resistance slightly. Based on the literature [29,36], it has been established that by the annealing scheme used in this study, the crystallinity of the as-anodized sample is increased. The formed crystalline NTs are believed to benefit from grains and grain boundaries acting as potential sites for the nucleation of a passive layer when exposed to corroding media [55,56], thereby improving the corrosion resistance Additionally, annealing can give rise to the further oxidation of the substrate in the NiTi/NT interface through the NT pathways and thereby to higher corrosion resistance. The PLGA-coated sample also shows the highest corrosion resistance compared to the other samples. The protective effect of polymer deposits on metallic substrates as a physical barrier against the access of the electrolyte has been previously corroborated [[57], [58], [59]], which is accompanied by a reduction in the leaching of metallic ions into the surrounding environment. This is beneficial for NiTi implants which impose a concern regarding the release of toxic and carcinogenic Ni ions into the surrounding tissue.

3.5. Cytocompatibility studies

The MTT assay was used to assess the DPSC cytocompatibility of the as-ground, as-anodized, vancomycin-loaded and vancomycin-loaded PLGA-coated samples (Fig. 8). On the first day, there is no significant difference between the cell viability of the samples, where all show suitable biocompatibility. In the study of Park et al. [37] on the analysis of focal contact formation of mesenchymal stem cells cultured on NTs with the diameter of 15–100 nm, it was shown that the

critical diameter of NTs for the best “integrin receptor” activation that is responsible for cell proliferation, migration, differentiation and survival is in the range of 15–30 nm. As indicated in Fig. 2, the NTs anodically-fabricated on NiTi in this study have a mean diameter of approximately 30 nm, which can explain the appropriate DPSCs viability on the related surface.

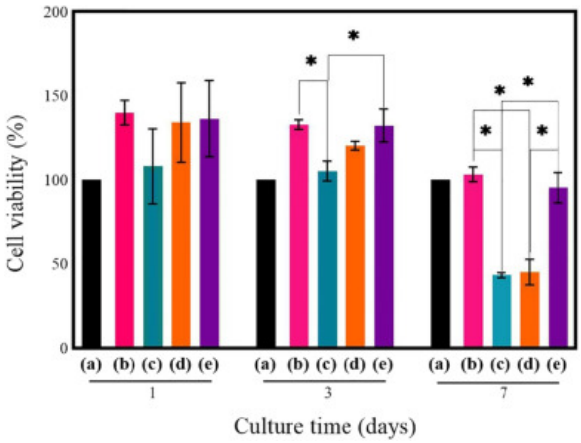

Fig. 8. Cell viability of the control (a), as-ground (b), as-anodized (c), vancomycin-loaded (d) and vancomycin-loaded PLGA-coated (e) samples, where * indicates significant difference with *p*-value < 0.05.

After three days of the cell culture, the as-anodized NTs show the lowest cell viability compared to the other samples, which could be due to the fact that this non-annealed sample suffers from toxic fluorine residuals on its surface. This finding is in agreement with previous studies on anodization of Ti alloys in fluorine-containing electrolytes [16]. This problem is overcome by annealing at above 500 °C [16,35], as the annealed NTs even after the drug loading present higher cytocompatibility than the as-anodized NTs in this study. The suitable cytocompatibility of the bare and PLGA-coated vancomycin-loaded NTs also suggests that the amount of vancomycin released until the third day is well tolerated by DPSCs. These findings are corroborated by previous studies in which a similar release dosage of vancomycin from NTs shows almost no negative effect on cell viability in vivo and in vitro [16].

On the 7th day of culture, the PLGA-coated drug-loaded NTs show the highest cell viability results. This finding is supported by other studies in which biocompatibility is improved by using PLGA as a barrier coating for the release of therapeutics [10,46,60]. The bare drug-loaded NTs show a significant reduction in cell viability in this time point, which might to be resulted from the excessive amount of vancomycin released from the device. This toxicity effect is consistent with studies conducted on local vancomycin-delivery systems in which excessive vancomycin leaching (>300–500 μg/ml) leads to cell death [50,61]. On the other hand, the controlled release of both vancomycin (Fig. 5) and metallic ions (Fig. 7) from the PLGA-coated sample is inferred to be well-tolerated by the cells, resulting in 95% cell viability at this time point. This verifies our hypothesis that PLGA coating of the NTs could control the release of vancomycin above its MIC value, while maintaining an upper-bound release dosage that does not reach vancomycin toxicity for DPSCs.

4. Conclusions

In this study, homogeneous open-top hydrophilic NTs are successfully fabricated on NiTi substrates by a sequence of the anodization, sonication and annealing processes, then loaded with vancomycin and

finally coated with PLGA. The coated NTs provide a modulated drug-delivery kinetics than the bare sample in terms of a reduced burst and prolonged total release within the therapeutic bound for osteomyelitis. Moreover, the PLGA coating contributes to the enhancement of corrosion resistance, and by extension to less metallic ions leaching of the substrate, which greatly enhances the DPSC cell viability compared to the bare samples.

CRediT authorship contribution statement

F. Davoodian: Conceptualization, Methodology, Validation, Formal analysis, Investigation, Resources, Writing - original draft. **E. Salahinejad:** Conceptualization, Methodology, Validation, Writing - review & editing, Supervision. **E. Sharifi:** Investigation, Resources, Writing - review & editing. **Z. Barabadi:** Investigation, Resources, Writing - review & editing. **L. Tayebi:** Resources, Writing - review & editing.

Declaration of competing interest

No conflict of interest.

References

[1] J. Ryhänen. **Biocompatibility of nitinol.** Minim. Invasive Ther. Allied Technol., 9 (2000), pp. 99-105

[2] S. Shabalovskaya, J. Van Humbeeck. **Biocompatibility of nitinol for biomedical applications.** Shape Memory Alloys for Biomedical Applications, Elsevier (2009), pp. 194-233

[3] S. Rahimipour, E. Salahinejad, E. Sharifi, H. Nosrati, L. Tayebi. **Structure, wettability, corrosion and biocompatibility of nitinol treated by alkaline hydrothermal and hydrophobic functionalization for cardiovascular applications.** Appl. Surf. Sci., 506 (2020), Article 144657

[4] M. McNally, K. Nagarajah. **(iv) Osteomyelitis.** Orthop. Trauma, 24 (2010), pp. 416-429

[5]W. Watters, M.P. Rethman, N.B. Hanson, E. Abt, P.A. Anderson, K.C. Carroll, H.C. Futrell, K. Garvin, S. O. Glenn, J. Hellstein. **Prevention of orthopaedic implant infection in patients undergoing dental procedures.** J. Am. Acad. Orthop. Surg., 21 (2013), pp. 180-189

[6] J.W. Costerton, P.S. Stewart, E.P. Greenberg. **Bacterial biofilms: a common cause of persistent infections.** Science, 284 (1999), pp. 1318-1322

[7] D.A. Wininger, R.J. Fass. **Antibiotic-impregnated cement and beads for orthopedic infections.** Antimicrob. Agents Chemother., 40 (1996), pp. 2675-2679

[8] B. Roeder, C.C. Van Gils, S. Maling. **Antibiotic beads in the treatment of diabetic pedal osteomyelitis.** J. Foot Ankle Surg., 39 (2000), pp. 124-130

[9] K. Gulati, S. Ramakrishnan, M.S. Aw, G.J. Atkins, D.M. Findlay, D. Losic. **Biocompatible polymer coating of titania nanotube arrays for improved drug elution and osteoblast adhesion.** Acta Biomater., 8 (2012), pp. 449-456

[10] W. Feng, Z. Geng, Z. Li, Z. Cui, S. Zhu, Y. Liang, Y. Liu, R. Wang, X. Yang. **Controlled release behaviour and antibacterial effects of antibiotic-loaded titania nanotubes.** Mater. Sci. Eng. C, 62 (2016), pp. 105-112

[11] S. Spriano, S. Yamaguchi, F. Baino, S. Ferraris. **A critical review of multifunctional titanium surfaces: new frontiers for improving osseointegration and host response, avoiding bacteria contamination.** Acta Biomater., 79 (2018), pp. 1-22

[12] M. Fathi, B. Akbari, A. Taheriazam. **Antibiotics drug release controlling and osteoblast adhesion from Titania nanotubes arrays using silk fibroin coating.** Mater. Sci. Eng. C, 103 (2019), Article 109743

[13] K.C. Popat, M. Eltgroth, T.J. LaTempa, C.A. Grimes, T.A. Desai. **Titania nanotubes: a novel platform for drug-eluting coatings for medical implants?** Small, 3 (2007), pp. 1878-1881

[14] Q. Wang, J.Y. Huang, H.Q. Li, Z. Chen, A.Z. Zhao, Y. Wang, K.Q. Zhang, H.T. Sun, S.S. Al-Deyab, Y.K. Lai. **TiO2 nanotube platforms for smart drug delivery: a review.** Int. J. Nanomedicine, 11 (2016), pp. 4819-4834

[15] A. Hamlekhan, S. Sinha-Ray, C. Takoudis, M.T. Mathew, C. Sukotjo, A.L. Yarin, T. Shokuhfar. **Fabrication of drug eluting implants: study of drug release mechanism from titanium dioxide nanotubes.** J. Phys. D. Appl. Phys., 48 (2015), Article 275401

[16] H. Zhang, Y. Sun, A. Tian, X.X. Xue, L. Wang, A. Alquhali, X. Bai. **Improved antibacterial activity and biocompatibility on vancomycin-loaded TiO2 nanotubes: in vivo and in vitro studies.** Int. J. Nanomedicine, 8 (2013), pp. 4379-4389

[17] D. Regonini, C.R. Bowen, A. Jaroenworaluck, R. Stevens. **A review of growth mechanism, structure and crystallinity of anodized TiO2 nanotubes.** Mater. Sci. Eng. R. Rep., 74 (2013), pp. 377-406

[18] R. Hang, Y. Liu, L. Zhao, A. Gao, L. Bai, X. Huang, X. Zhang, B. Tang, P.K. Chu. **Fabrication of Ni-Ti-O nanotube arrays by anodization of NiTi alloy and their potential applications.** Sci. Rep., 4 (2014), p. 7547

[19] S. Grigorescu, V. Pruna, I. Titorencu, V.V. Jinga, A. Mazare, P. Schmuki, I. Demetrescu. **The two step nanotube formation on TiZr as scaffolds for cell growth.** Bioelectrochemistry, 98 (2014), pp. 39-45

[20] J.-H. Kim, K. Zhu, Y. Yan, C.L. Perkins, A.J. Frank. **Microstructure and pseudocapacitive properties of electrodes constructed of oriented NiO-TiO2 nanotube arrays.** Nano Lett., 10 (2010), pp. 4099-4104

[21] F. Mohammadi, M. Kharaziha, A. Ashrafi. **Role of heat treatment on the fabrication and electrochemical property of ordered TiO2 nanotubular layer on the as-cast NiTi.** Met. Mater. Int., 25 (2018), pp. 617-626

[22] R. Hang, Y. Liu, S. Liu, L. Bai, A. Gao, X. Zhang, X. Huang, B. Tang, P.K. Chu. **Size-dependent corrosion behavior and cytocompatibility of Ni–Ti–O nanotubes prepared by anodization of biomedical NiTi alloy.** Corros. Sci., 103 (2016), pp. 173-180

[23] R. Qin, D.Y. Ding, C.Q. Ning, H.G. Liu, B.S. Zhu, M. Li, D.L. Mao. **Ni-doped TiO2 nanotube arrays on shape memory alloy.** Appl. Surf. Sci., 257 (2011), pp. 6308-6313

[24]M.J. Rybak, B.M. Lomaestro, J.C. Rotschafer, R.C. Moellering, W.A. Craig, M. Billeter, J.R. Dalovisio, D.P. Levine. **Vancomycin therapeutic guidelines: a summary of consensus recommendations from the infectious diseases Society of America, the American Society of Health-System Pharmacists, and the Society of Infectious Diseases Pharmacists.** Clin. Infect. Dis., 49 (2009), pp. 325-327

[25] P. Gentile, V. Chiono, I. Carmagnola, P.V. Hatton. **An overview of poly(lactic-co-glycolic) acid (PLGA)-based biomaterials for bone tissue engineering.** Int. J. Mol. Sci., 15 (2014), pp. 3640-3659

[26] H.K. Makadia, S.J. Siegel. **Poly lactic-co-glycolic acid (PLGA) as biodegradable controlled drug delivery carrier.** Polymers (Basel), 3 (2011), pp. 1377-1397

[27] M Körber. **PLGA erosion: solubility-or diffusion-controlled?** Pharm. Res., 27 (2010), pp. 2414-2420

[28] Y. Liu, Z. Ren, L. Bai, M. Zong, A. Gao, R. Hang, H. Jia, B. Tang, P.K. Chu. **Relationship between Ni release and cytocompatibility of Ni-Ti-O nanotubes prepared on biomedical NiTi alloy.** Corros. Sci., 123 (2017), pp. 209-216

[29] R. Hang, X. Huang, L. Tian, Z. He, B. Tang. **Preparation, characterization, corrosion behavior and bioactivity of Ni2O3-doped TiO2 nanotubes on NiTi alloy.** Electrochim. Acta, 70 (2012), pp. 382-393
[30] X. Huang, Y. Liu. **Effect of annealing on the transformation behavior and superelasticity of NiTi shape memory alloy.** Scr. Mater., 45 (2001), pp. 153-160
[31] G. Satoh, A. Birnbaum, Y.L. Yao. **Annealing effect on the shape memory properties of amorphous NiTi thin films.** J. Manuf. Sci. Eng., 132 (2010), Article 051004
[32] R. Byrne, P. Deasy. **Use of commercial porous ceramic particles for sustained drug delivery.** Int. J. Pharm., 246 (2002), pp. 61-73
[33] S. Karimi, E. Salahinejad, E. Sharifi, A. Nourian, L. Tayebi. **Bioperformance of chitosan/fluoride-doped diopside nanocomposite coatings deposited on medical stainless steel.** Carbohydr. Polym., 202 (2018), pp. 600-610
[34] H. Xu, Q. Zhang, C. Zheng, W. Yan, W. Chu. **Application of ultrasonic wave to clean the surface of the TiO2 nanotubes prepared by the electrochemical anodization.** Appl. Surf. Sci., 257 (2011), pp. 8478-8480
[35] B. Ercan, E. Taylor, E. Alpaslan, T.J. Webster. **Diameter of titanium nanotubes influences anti-bacterial efficacy.** Nanotechnology, 22 (2011), Article 295102
[36] Q. Liu, D. Ding, C. Ning. **Anodic fabrication of Ti-Ni-O nanotube arrays on shape memory alloy.** Materials, 7 (2014), pp. 3262-3273
[37] J. Park, S. Bauer, K. von der Mark, P. Schmuki. **Nanosize and vitality: TiO2 nanotube diameter directs cell fate.** Nano Lett., 7 (2007), pp. 1686-1691
[38] G.-Y. Hou, Y.-Y. Xie, L.-K. Wu, H.-Z. Cao, Y.-P. Tang, G.-Q. Zheng. **Electrocatalytic performance of Ni-Ti-O nanotube arrays/NiTi alloy electrode annealed under H2 atmosphere for electro-oxidation of methanol.** Int. J. Hydrog. Energy, 41 (2016), pp. 9295-9302
[39] F. Mohammadi, N. Golafshan, M. Kharaziha, A. Ashrafi. **Chitosan-heparin nanoparticle coating on anodized NiTi for improvement of blood compatibility and biocompatibility.** Int. J. Biol. Macromol., 127 (2019), pp. 159-168
[40] Q. Wang, J.-Y. Huang, H.-Q. Li, A.Z.-J. Zhao, Y. Wang, K.-Q. Zhang, H.-T. Sun, Y.-K. Lai. **Recent advances on smart TiO2 nanotube platforms for sustainable drug delivery applications.** Int. J. Nanomedicine, 12 (2017), pp. 151-165
[41] S. Ferraris, A. Bobbio, M. Miola, S. Spriano. **Micro-and nano-textured, hydrophilic and bioactive titanium dental implants.** Surf. Coat. Technol., 276 (2015), pp. 374-383
[42] C. Chu, R. Wang, L. Yin, Y. Pu, P. Lin, Y. Dong, C.Y. Chung, K. Yeung, P. Chu. **Effects of anodic oxidation in H2SO4 electrolyte on the biocompatibility of NiTi shape memory alloy.** Mater. Lett., 62 (2008), pp. 3512-3514
[43] G. Liu, K. Du, K. Wang. **Surface wettability of TiO2 nanotube arrays prepared by electrochemical anodization.** Appl. Surf. Sci., 388 (2016), pp. 313-320
[44] K.C. Popat, M. Eltgroth, T.J. LaTempa, C.A. Grimes, T.A. Desai. **Titania nanotubes: A novel platform for drug-eluting coatings for medical implants?.** Small, 3 (2017), pp. 1878-1881
[45] K.C. Yan Hu, Zhong Luo Dawei Xu, Daichao Xie Yuran Huang, Weihu Yang Peng Liu. **Titania nanotube arrays for local drug delivery recent advances and perspectives.** Acta Biomater., 8 (2011), pp. 439-448
[46] M.S. Aw, K. Gulati, D. Losic. **Controlling drug release from titania nanotube arrays using polymer nanocarriers and biopolymer coating.** J. Biomater. Nanobiotechnology, 2 (2011), pp. 477-484
[47] S. Karki, H. Kim, S.-J. Na, D. Shin, K. Jo, J. Lee. **Thin films as an emerging platform for drug delivery.** Asian J. Pharm. Sci., 11 (2016), pp. 559-574

[48] T.T.D. Tran, P.H.L. Tran. **Controlled release film forming systems in drug delivery: the potential for efficient drug delivery.** Pharmaceutics, 11 (2019), p. 290
[49] C. Loc-Carrillo, C. Wang, A. Canden, M. Burr, J. Agarwal. **Local intramedullary delivery of vancomycin can prevent the development of long bone Staphylococcus aureus infection.** PLoS One, 11 (2016), Article e0160187
[50] V. Antoci Jr., C.S. Adams, N.J. Hickok, I.M. Shapiro, J. Parvizi. **Antibiotics for local delivery systems cause skeletal cell toxicity in vitro.** Clin. Orthop. Relat. Res., 462 (2007), pp. 200-206
[51] J. Siepmann, F. Siepmann. **Modeling of diffusion controlled drug delivery.** J. Control. Release, 161 (2012), pp. 351-362
[52] P. Costa, J.M.S. Lobo. **Modeling and comparison of dissolution profiles.** Eur. J. Pharm. Sci., 13 (2001), pp. 123-133
[53] S. Dash, P.N. Murthy, L. Nath, P. Chowdhury. **Kinetic modeling on drug release from controlled drug delivery systems.** Acta Pol. Pharm., 67 (2010), pp. 217-223
[54] L. Peng, A.D. Mendelsohn, T.J. LaTempa, S. Yoriya, C.A. Grimes, T.A. Desai. **Long-term small molecule and protein elution from TiO2 nanotubes.** Nano Lett., 9 (2009), pp. 1932-1936
[55] M. Chembath, J.N. Balaraju, M. Sujata. **Effect of anodization and annealing on corrosion and biocompatibility of NiTi alloy.** Surf. Coat. Technol., 302 (2016), pp. 302-309
[56] T. Hu, Y. Xin, S. Wu, C. Chu, J. Lu, L. Guan, H. Chen, T.F. Hung, K. Yeung, P.K. Chu. **Corrosion behavior on orthopedic NiTi alloy with nanocrystalline/amorphous surface.** Mater. Chem. Phys., 126 (2011), pp. 102-107
[57] J. Szewczenko, W. Kajzer, M. Grygiel-Pradelok, J. Jaworska, K. Jelonek, K. Nowińska, M. Gawliczek, M. Libera, A. Marcinkowski, J. Kas perczyk. **Corrosion resistance of PLGA-coated biomaterials.** Acta Bioeng. Biomech., 19 (2017), pp. 173-179
[58]W. KAjzer, J. Jaworska, K. Jelonek, J. Szewczenko, A. Kajzer, K. Nowińska, A. Hercog, M. Kaczmarek, J. Kasperczyk. **Corrosion resistance of Ti6Al4V alloy coated with caprolactone-based biodegradable polymeric coatings.** Eksploatacja i Niezawodnosc - Maintenance and Reliability, 20 (2018), pp. 30-38
[59] S. Rastegari, E. Salahinejad. **Surface modification of Ti-6Al-4V alloy for osseointegration by alkaline treatment and chitosan-matrix glass-reinforced nanocomposite coating.** Carbohydr. Polym., 205 (2019), pp. 302-311
[60] T. Kumeria, H. Mon, M.S. Aw, K. Gulati, A. Santos, H.J. Griesser, D. Losic. **Advanced biopolymer-coated drug-releasing titania nanotubes (TNTs) implants with simultaneously enhanced osteoblast adhesion and antibacterial properties.** Colloids Surf. B: Biointerfaces, 130 (2015), pp. 255-263
[61] C.R. Rathbone, J.D. Cross, K.V. Brown, C.K. Murray, J.C. Wenke. **Effect of various concentrations of antibiotics on osteogenic cell viability and activity.** J. Orthop. Res., 29 (2011), pp. 1070-1074